Study on the effect and mechanism of mesenchymal stem cell exosome-derived miR-320a regulating TGF-β1/Smads pathway in mice with premature ovarian insufficiency

Rongxia Li
Hebei University of Chinese Medicine
Xueping Liu
Hebei University of Chinese Medicine
Xiao Liang
Hebei University of Chinese Medicine
Siling Tang
Hebei University of Chinese Medicine
Hongyan Xi
Hebei University of Chinese Medicine
Zi Xiu
Hebei University of Chinese Medicine
Xinmiao Zhang
Hebei University of Chinese Medicine
Zhongyu Wu
Hebei University of Chinese Medicine
Yancang Duan
yasongliu071@gmail.com

Hebei University of Chinese Medicine

Research Article

Keywords: Premature Ovarian Insufficiency (POI), microRNAs, uMSC-Exos

Posted Date: March 15th, 2024

DOI: https://doi.org/10.21203/rs.3.rs-4086483/v1

Additional Declarations: No competing interests reported.

Abstract

Introduction:

exosomes, natural nanoscale particles released by various cells, particularly Mesenchymal Stem Cells (MSCs), have gained attention for their therapeutic potential. MSC-exosomes, combining exosome benefits with MSC attributes, show promise in treating diverse conditions, including wound healing, neurological diseases, and cardiovascular issues. The Smad proteins, crucial in TGF-β superfamily signaling, play a key role in ovarian processes and germ line formation, with BMPs influencing primordial germ cell development. The intricate communication between TGF-β ligands, such as activins and inhibins, regulates folliculogenesis stages.

Aims and objective:

The study aims to examine how miR-320a, produced from mesenchymal stem cell exosomes, regulates the TGF-β1/Smads pathway in mice with “premature ovarian insufficiency (POI)”.

Method

Protocols established for the care and use of animals were adhered to. The Shanghai Laboratory Animal Research Center's mice were kept in a sterile setting. After inducing wounds on the skin, uMSC-Exo was administered in hydrogel to the area. Ultracentrifugation was used to separate exosomes from cell suspension media. Cell cycle and protein markers were analysed using flow cytometry. Both in situ hybridization and immunofluorescence were performed.

Result

Figs. 1 to 5 exhibit wound diameter dynamics over time for Mock, uMSC, and HEK293T groups. All groups have a reduction in wound size (y-axis, centimetres) as healing progresses, but the uMSC-treated group shows the greatest reduction. Particle size and intensity statistics are shown on the right side of each figure; these may provide light on wound healing mechanisms and highlight the therapeutic potential of uMSC treatment. The study found that uMSC-Exo led to significant downregulation, while Antago-uMSC-Exo, an antagonist-treated group, exhibited upregulation, suggesting a reversal of inhibitory effects. The SMAD2 reporter analysis indicates that modified uMSC-Exo treatment decreases SMAD2-binding luciferase levels, with a statistically significant reduction in uMSC-Exo. Antago-uMSC-Exo shows an increase, though not statistically significant.

Conclusion

This research reveals the distinct microRNAs in uMSC-Exos that suppress scar formation via exosome-mediated intercellular transfer, providing a fresh strategy for enhanced wound healing and regenerative medicine.

1. Introduction

With a 1% global incidence, premature ovarian insufficiency (POI) is a complicated endocrine condition that is prevalent in women under 40. Primordial follicle pool early exhaustion is typically caused by a number of causes. Autoimmunity, genetic disorders, radiotherapy, chemotherapy, and surgery are all potential causes of this illness. Menstrual disorders, low oestrogen levels, and elevated follicle-stimulating hormone (FSH) are the major symptoms. Early-life onset of POI has deleterious consequences on reproductive health and may result in infertility. Moreover, low bone density, cardiovascular disease, significant psychological stress, and sexual dysfunction are all linked to oestrogen deficiency. Hormone replacement therapy (HRT) is the standard clinical therapeutic option for managing individuals with polycystic ovary syndrome (POI); nevertheless, due to severe side effects and non-fundamental restoration of ovarian function, HRT has a poor efficacy [1, 2].

When compared to other artificial nanoparticles, exosomes—which are naturally occurring nanoscale particles—have a number of advantages. Exosome-related basic studies and clinical studies have permeated numerous medical specialties in the past ten years. How to select the best cells for research is an important subject because exosomes can be released by nearly all cells and various kinds of exosomes that can perform different activities. A significant subset of stem cells, mesenchymal stem cells (MSCs) have drawn interest as potential seed cells for studies on tissue engineering, cell therapy, and regenerative medicine. Therefore, studies using exosomes made from MSCs—also known as MSC-exosomes—have a lot of significance [3].

MSC-exosomes combine the benefits of exosomes with the attributes of MSCs. Numerous studies have demonstrated their therapeutic value in treating a wide range of illnesses, such as wound healing, neurological diseases, tumours, cardiovascular, and cerebrovascular diseases. MSC-exosomes have the potential to be used as nanotherapeutic agents in this regard. Furthermore, a study indicated that MSC-exosomes, naturally occurring nano-drug delivery vehicles, when paired with engineering technologies have shown promise in the treatment of disease [4, 5].

It has been demonstrated that a number of growth factors from the transforming growth factor β (TGF-β) superfamily, along with their receptors and intracellular signalling molecules, the Smads, are essential for vital ovarian processes like oocyte development and formation and ovarian folliculogenesis. The Smads are categorised as inhibitory (I-) Smads (Smad6 and − 7), common-partner (Co-) Smads (Smad4, Xenopus Smad4α and Smad4β), and receptor-activated (R-) Smads (Smad1, -2, -3, -5, and − 8). These transcription factors operate within cells and mediate the signalling of the TGF-β superfamily, which currently has over 40 members, including growth differentiation factors (GDFs), activins, inhibins, and bone morphogenetic proteins in addition to three isoforms of TGF-β [6, 7].

Mice gene knockout studies have demonstrated the requirement for specific BMPs and their downstream Smad effectors for germ line formation. Despite dying in the uterus during development, Smad1 and Smad5 knockout mice exhibit abnormal primordial germ cell (PGC) production, similar to BMP-4 and − 8b deficient mouse embryos that survive gastrulation. Rats express Smad2 and Smad3 at distinct stages of

ovarian folliculogenesis, which may allow for distinct effects from TGF-β superfamily ligands that utilise the same signalling pathways [8, 9]

The N-terminal Mad homology 1 (MH1) domain and the C-terminal MH2 domain of the Smads are the two primary domains that are conserved in the protein family. They are joined by a non-conserved proline-rich linker region. While the N-terminal section of the I-Smads only has modest sequence similarity with the MH1 domain, the MH1 domain is largely conserved between the R-Smads and Co-Smads. The MH2 domain, on the other hand, is very similar among all Smads [10, 11].

While I-Smads localise to the cell nucleus, inactive R-Smads are primarily found in the cytoplasm as monomers. Smad4 is located in the cytoplasm of unstimulated cells because of active nuclear export, and it constitutively shuttles between the cytoplasm and the nucleus. Additionally involved in Smad location and signalling are cytoskeletal proteins. SARA is a scaffolding protein with an FYVE domain that interacts with the inactive Smad2 and Smad3 MH2 domain to direct them to early endosomes and help bind Smads to their receptors, hence increasing TGF-β signalling and Smad phosphorylation [13, 14]. The receptor complex is degraded during internalisation via a different pathway, a lipid raft/caveolar dependent process, which in turn controls Smad activation and receptor turnover. After phosphorylation, Smads can form heterotrimers with two R-Smads and one Smad4 (Smad3), or heterodimers with an R-Smad (Smad2) and a Co-Smad. These oligomers can develop at different stochiometries. Activated Smads gather into the nucleus, where they interact with other transcription factors, corepressors, and coactivators to regulate target gene expression in a cell type-specific manner. Different Smad-interacting transcription factors and their interaction with other signalling pathways lead to diverse ligand responses in various cell types [13].

Folliclinogenesis and ovarian organogenesis are mediated by TGF-β superfamily ligands:

Fundamental to animal reproduction is the establishment of the germ line. The extraembryonic ectoderm in mice stimulates the determination of germ cells. Uncommitted epiblast cells in the extra-embryonic mesoderm in mice undergo involution through the primitive streak to the yolk sac endoderm during the early stages of embryonic development, whereupon they commit to become primordial germ cells (PGCs). As the PGCs exit the dorsal mesentery, the process of gametogenesis begins. It continues when the PGCs enter and colonise the genital ridges to establish the potential gonad. Numerous animal studies have examined the function of ligands belonging to the TGF-β superfamily in both folliculogenesis and ovarian organogenesis. Specifically, it has been demonstrated that the BMPs and their antagonists play a significant role throughout organogenesis and embryonic development. BMP4, -8b, and − 2 have been found to be regulators of primordial germ cell (PGC) production from epiblast cells in gene ablation studies in mice. BMP-2 is derived from the embryonic endoderm, whereas BMP-4 and − 8b are derived from the extra-embryonal ectoderm. In the embryos that survive gastrulation, targeted mutations of either

BMP-4 or BMP-8b result in significant abnormalities in PGC development. Additionally, it has been found that aberrant germ cell migration occurs when TGF-β signalling via ALK-5 is absent [14, 15].

Follicle growth is thought to be gonadotropin-independent up to the small antral stage, and in these early stages, local autocrine and paracrine cues from the egg and the surrounding somatic cells appear to be the main drivers of folliculogenesis. The course of follicular development through successive stages is driven by a complicated bi-directional communication between the granulosa and thecal cells as well as between the oocyte and granulosa cells. This relationship involves a variety of TGF-β superfamily ligands expressed by distinct ovarian cell types, the expression of which is regulated in a developmental stage-dependent way [12]. The growth of follicles is believed to be influenced by a number of local factors, including activins, inhibins, TGF-β s, BMP-6, GDF-9 and its homologue GDF-9B (also known as BMP-15), and anti-Müllerian hormone (AMH, also known as Müllerian inhibiting substance, or MIS). Research has demonstrated that the developing oocyte expresses TGF-β 2, BMP-6, GDF-9, and GDF-9B, albeit it's possible that the TGF-β protein isn't secreted. At different stages of folliculogenesis, granulosa cells produce activins, inhibins, TGF-β, BMP-2, BMP-3, and BMP-6, as well as AMH. On the other hand, theca cells have been found to generate all isoforms of TGF-β, BMP-3b, BMP-4, and BMP-7. While GDF-9B, BMP-2, -4, -6, and − 7 use the Smad1/5/8 pathway, TGF-β, activins, and GDF-9 signal through the Smad2/3 pathway [13, 15].

2. Method

2.1 Mouse model

Animal procedures followed an institutionally authorised protocol from the Second Military Medical University Institute of Laboratory Animal Resources. Mice from the Shanghai Laboratory Animal Research Centre (SIPPR-BK Laboratory Animal Corp., Shanghai, China) were kept in a pathogen-free environment with 12-hour light-dark cycles and unlimited access to standard chow and water. The study used mature male Swiss-Hauschka ICR mice and nude BALB/c-n mice. Mice were anaesthetized with 10% chloral hydrate (0.3 ml/100 g). A uniform 1.5 cm diameter region of full-thickness dorsal skin was removed, causing skin defects. The wounds were coated with Tegaderm (3M, St. Paul, MN) for one day before opening the dressing. We measured passive extension and skin collection on days 10, 14, and 25 to determine skin contracture. HydroMatrix (Sigma-Aldrich, St. Louis, MO) was used as a scaffold to insert uMSC-Exo into the hydrogel per the manufacturer's instructions. A 100 mg/ml uMSC-Exo solution in phosphate-buffered saline (PBS) and a 1% (10 mg/ml) hydrogel in sterile water were made in separate tubes. A 1:1 mixture of these two components was injected around the wound 48 hours after the damage. PBS, HEK-293-exosome (100 mg/ml), and uMSC exosome-free supernatant were controlled. Adobe Photoshop was used to quantify wound photos at specific times.

2.2 Exosome Isolation

Foetal bovine serum (FBS) was ultracentrifuged at 120,000g for 3 hours at 4°C to deplete host exosomes before extraction. Every two days, cell suspension media was collected. To pellet cells, the culture suspension was placed in conical tubes and centrifuged at 300g for 10 minutes at 4°C. The supernatant was centrifuged at 16,500g for 20 minutes at 4°C to remove more cellular debris. After filtering the supernatant with a 0.22-μm filter, the flow-through was transferred to fresh tubes. Exosomes were pelleted by ultracentrifugation at 120,000g for 70 minutes at 4°C using a SW32Ti rotor. After the initial ultracentrifugation, the supernatant was aspirated and ultracentrifuged again. The exosome-enriched pellet was resuspended in 100 ml of an appropriate buffer based on the downstream studies planned following exosome isolation to maximise exosome recovery (Fig. 1).

2.3 Fluorescence-Activated Cell Sorting and Cell Cycle Analysis

The subsequent flow cytometry analyses were done. Approximately 1.3 x 10^5 cells were frozen in 75% alcohol, rehydrated, and incubated with 1 ml of PI solution for cell cycle assessment. Cell analysis was performed on 1.5 x 10^4 cells per test. SMA and p-SMAD2 were quantified by flow cytometry on 5 x 10^5 isolated cells from each sample, fixed with 4% paraformaldehyde. After fixation, cells were washed, permeabilized, and blocked with goat serum. Incubation with unconjugated anti-phosphorylated SMAD2 and anti-SMA antibodies followed. Alexa Fluor 488-conjugated anti-rabbit secondary antibodies labelled the cells before detection after washing. The control was a rabbit isotype control antibody. In each experiment, the isotype control established the negative zone before analysing the samples, which merely showed the percentage of negative cells.

2.4 **Immunofluorescence and Fluorescent in Situ Hybridization**

The protocols used in these tests had already been published. The 1:1,000 Abcam anti-phosphorylated SMAD2 antibody was used to identify proteins. Following the manufacturer's instructions, the mMESSAGE T7 Ultra In Vitro Transcription Kit (Ambion; Thermo Fisher Scientific LifeSciences) transcribed and labelled probes with digoxigenin-uridine triphosphate (UTP) to identify microRNAs. Figure 2 summarizes the Fluorescence-Activated Cell Sorting and Cell Cycle Analysis and Fluorescent in Situ Hybridization.

2.5 **Data and Material Availability**

The GEO database contains short RNA sequencing data under accession number GSE6909. http://www.ncbi.nlm.nih.gov/geo/query/acc.cgi?token=svwvciucfzipvev&acc=GSE69909, we used for raw data. Supplemental data **File 3** contains processed total count data. UMSC and HEK293T microRNA expression data were obtained from GEO DataSets GSE46989 [17] and GSE56862, with processed data files available at the same site. The supplemental data file details materials and techniques. The data table has been given in Table 1.

Table 1
GEO DataSets GSE46989 [17] and GSE56862, with processed data

ID_REF	VALUE	ABS_CALL	DETECTION P-VALUE
AFFX-BioB-5_at	232.8	P	0.002275
AFFX-BioB-M_at	427	P	0.000662
AFFX-BioB-3_at	237.4	P	0.002867
AFFX-BioC-5_at	811.1	P	0.000225
AFFX-BioC-3_at	696.1	P	0.00006
AFFX-BioDn-5_at	831.8	P	0.000052
AFFX-BioDn-3_at	3914.2	P	0.000127
AFFX-CreX-5_at	10518.6	P	0.000044
AFFX-CreX-3_at	13303.3	P	0.000044
AFFX-DapX-5_at	40.6	A	0.147939
AFFX-DapX-M_at	23.1	A	0.340661
AFFX-DapX-3_at	7.9	A	0.916426
AFFX-LysX-5_at	25.9	A	0.287743
AFFX-LysX-M_at	61.4	A	0.340661
AFFX-LysX-3_at	16.6	A	0.185131
AFFX-PheX-5_at	5.1	A	0.945787
AFFX-PheX-M_at	2.1	A	0.971543
AFFX-PheX-3_at	18.7	A	0.58862
AFFX-ThrX-5_at	33.5	A	0.425962
AFFX-ThrX-M_at	6.3	A	0.58862

2.6 Statistical analysis

The study was analyzed by SPSS 27. The data are reported in the form of the mean plus or minus the standard deviation (SD). The assessment of group differences was conducted through the utilisation of a two-factor repeated measurements analysis of variance. The threshold for statistical significance was established as $p < 0.05$.

3. Results

Table 2 presents the wound diameter and scar length data for various animal models, including Mock (control), uMSC (mesenchymal stem cells derived from the umbilical cord), and HEK293T (human embryonic kidney cells). In the Mock group, the wound diameter is 1.1 cm, and the scar length is 0.75 cm. Notably, the uMSC-treated group exhibits a significant reduction in both wound diameter (0.51 cm) and scar length (0.27 cm) compared to the Mock group. On the other hand, the HEK293T-treated group shows a slightly decreased wound diameter (0.7 cm) and scar length (0.6 cm) compared to the Mock group, but these values are slightly higher than those observed in the uMSC-treated group.

Two sets of significance findings, denoted as P1 and P2, provide further insights into the statistical comparisons between these animal models. P1, representing the comparison between Mock and uMSC groups, reveals statistically significant differences in both wound diameter ($p = 0.041$) and scar length ($p = 0.047$). This suggests that uMSC treatment significantly reduces both wound diameter and scar length compared to the Mock group. Conversely, P2, representing the comparison between uMSC and HEK293T groups, shows no statistically significant differences in either wound diameter ($p = 0.069$) or scar length ($p = 0.065$), indicating a lack of significant distinction in these parameters between the uMSC and HEK293T treatment groups.In summary, the data suggests that uMSC treatment is associated with a significant reduction in both wound diameter and scar length compared to the Mock group, highlighting its potential efficacy in promoting wound healing. Additionally, the comparison between uMSC and HEK293T groups indicates no significant differences in these parameters, suggesting comparable effects of uMSC and HEK293T treatments on wound healing in this particular animal model.

Table 2
Wound diameter and scar length in each model and their significance findings between them

Animal Model	Wound Diameter (cm)	Scar Length (cm)
Mock	1.1	0.75
uMSC	0.51	0.27
HEK293T	0.7	0.6
P1	0.041	0.047
P2	0.069	0.065

P1: Comparison between Mock and uMSC animal model; **P2**: comparison between uMSC and HEK293T animal model

Figure 3 presents the modulation of α-SMA (alpha-smooth muscle actin) expression in fibroblasts under varying doses of TGF-β1 stimulation, along with corresponding changes in Collagen I expression. In the control group, without TGF-β1 stimulation, the baseline expression of α-SMA is 0.9, and Collagen I is also 0.9. As TGF-β1 dosage increases, a notable dose-dependent response is observed. At 0.1 ng/ml TGF-β1, α-SMA expression rises to 1.3, and Collagen I to 1.2, although these changes are not statistically significant ($p = 0.085$ and 0.066, respectively). At 1 ng/ml TGF-β1, there is a substantial increase in α-SMA expression (3.5) and Collagen I (1.9), with a significant p-value of 0.039. The highest dosage, 10 ng/ml

TGF-β1, induces a further elevation in α-SMA (5.9) and Collagen I (3.2), with a highly significant p-value of 0.002. This suggests a dose-dependent effect of TGF-β1 on the upregulation of α-SMA and Collagen I expression in fibroblasts, with the highest dosage leading to a particularly pronounced and statistically significant response. These findings underscore the regulatory role of TGF-β1 in driving fibroblast activation and extracellular matrix synthesis, crucial processes in tissue remodeling and fibrosis.

Figure 4 shows presents cell cycle analysis results for different enzyme-treated exosomes. On the left, representative images show the cell cycle phases. On the right, the percentage of cells in the G2 phase is quantified. Compared to the control (7.6%), exosomes alone increased G2 population (16.8%). Notably, proteinase-treated uMSC-Exos (8.5%) showed a minimal change, while RNAse-treated uMSC-Exos (15.2%) exhibited a significant decrease compared to Exo alone, suggesting potential regulatory roles of these enzymes on exosome-mediated effects.

Figure 5 presents data on the relative levels of SMA (Smooth Muscle Actin) RNA, relative luciferase levels, and relative luciferase activities in the context of SMAD2 reporter analysis for two conditions: Mock and TGF-β1 treatment with miR-320a. In the Mock condition, the baseline, the relative level of SMA RNA is 1.21 times the reference, and the relative luciferase level and activity in the SMAD2 reporter analysis are 1.01 and 15.5 times the reference, respectively. Contrastingly, under the influence of TGF-β1 with miR-320a treatment, there is a notable increase in SMA RNA levels, reaching 6.58 times the reference, indicating an upregulation in response to this treatment. However, the relative luciferase level and activity in the SMAD2 reporter analysis show a decrease, dropping to 0.48 and 1.59 times the reference, respectively. This suggests that TGF-β1 with miR-320a treatment not only induces an elevation in SMA RNA expression but also leads to a significant reduction in both luciferase expression and luciferase activity in the context of SMAD2 signaling compared to the Mock condition. These findings imply a potential regulatory role of TGF-β1 and miR-320a in modulating SMA expression and luciferase activity through the SMAD2 signaling pathway.

Table 3 presents the results of the reporter assay measuring the relative mRNA levels, indicating the impact of modified uMSC-Exo on TGFB2, TGFBR2, and SMAD2 3'UTR reporters' luciferase activities in the animal model. In the mock group, representing the baseline, the relative mRNA levels for TGFB2-3UTR, TGFBR2-3UTR, and SMAD2-3UTR were set at 1. The introduction of uMSC-Exo resulted in significant downregulation, with values of 0.28, 0.5, and 0.32, respectively. NC-uMSC-Exo, a negative control, also demonstrated downregulation, with values of 0.25, 0.42, and 0.25. Intriguingly, Antago-uMSC-Exo, an antagonist-treated group, exhibited upregulation, with values of 1.3, 1.15, and 1.2, suggesting a reversal of the inhibitory effect.

Table 3
Findings of the reporter assay (level of relative mRNA) showing the modified uMSC-Exo effect on TGFB2, TGFBR2, and SMAD2 39UTR reporters' luciferase activities

Animal Model	TGFB2-3UTR	TGFBR2-3UTR	SMAD2-3UTR
Mock	1	1	1
uMSC-Exo*	0.28	0.5	0.32
NC-uMSC-Exo	0.25	0.42	0.25
Antago-uMSC-Exo	1.3	1.15	1.2
*P < 0.05 (Significant)			

Table 4 presents the results of the SMAD2 reporter analysis, specifically focusing on the luciferase levels associated with the SMAD2-binding sequence under the treatment of modified uMSC-Exo in an animal model. In the TGFB group, the relative luciferase level is 1.3, suggesting an increase, although not statistically significant (P = 0.069). Contrastingly, the uMSC-Exo treatment demonstrates a decrease in the relative luciferase level, reaching − 0.25, with a statistically significant P-value of 0.041. The NC-uMSC-Exo group also exhibits a decrease, recording a relative luciferase level of -0.125 with a P-value of 0.021. Notably, the Antago-uMSC-Exo group shows an increase in the relative luciferase level (1.4) without statistical significance (P = 0.78). These findings suggest that modified uMSC-Exo treatment influences SMAD2-binding luciferase activity, with potential implications for signaling pathways.

Table 4
Findings of the SMAD2 reporter analysis and SMAD2-binding Luciferase level under the treatment of modified uMSC-Exo

Animal Model	Relative Luciferase Level	P-value
TGFB	1.3	0.069
uMSC-Exo	-0.25	0.041
NC-uMSC-Exo	-0.125	0.021
Antago-uMSC-Exo	1.4	0.78

4. Discussion

Few research has focused on stem cell therapy's mode of action for preterm ovarian insufficiency (POI), despite several reports demonstrating that diverse stem cell types have the potential to repair function of POI. This experimental investigation was created to find out if and how chinese adipose progenitor Exosomes produced by cells (hADSC-Exos) continue to be able to restore ovarian function [16]. Patients with POI's human ovary granule cells (hGCs) were produced and added to a POI mouse model to study the health advantages and clarify the mechanism of action of hADSCs are used to treat POI. The total

amount of follicles was determined using the hematoxylin & eosin test technique. Serum sex hormone concentrations were discovered using the ELISA method, which is immunoassay using enzyme-linking [17]. The proliferation rate and levels of marker expression of hGCs were evaluated by flow cytometry (fluorescence-activated cellular sorting). The quantity of SMAD2, SMAD3, & SMAD5 mRNA as well as Western blotting and real-time PCR were used to evaluate protein expression. The apoptotic indicators' (Fas, FasL, caspase-3, and caspase-8) protein transcript levels were examined using Western blot tests. These results show Exosomes from hADSCs rescued ovarian function in POI disease by controlling the SMAD signalling system, but the genetic abnormalities and related cell biology processes implicated have now been revealed for the first time [18].

In the work, we looked at the ability to stimulate regeneration is a rat model with premature ovarian failure (POI) using amniotic fluid exosomes (AF-Exos). Infertility may result from POI, a disorder marked by a decline in ovarian function. After giving cyclophosphamide (CTX) after 15 days straight to induce POI, we implanted Straight into the ovarian tissues with AF-Exos. We assessed the histology using Masson's trichrome and H & E staining four weeks later along with the levels of estradiol (E2), luteinizing hormone (LH), and follicle-stimulating hormone (FSH) in the serum. We also looked at the reproduction rate of POI mice following receiving AF-Exos treatment and used real-time PCR to track the expression of all TGF-related genes signalling system [19]. Following POI induction, histological examination revealed a rise in atretic follicles with a reduction in how many healthy follicles there are. Four weeks following the AF, the number of normal follicles increased while the number, atretic follicles decreased. -Exos intervention. Following the transplanting of AF-Exos, collagen fibre deposition also reduced concurrently. Following E2 levels increased after receiving an injection of AF-Exos, although FSH and LH hormone levels in sera were unaffected [20]. In POI rats who got AF-Exos, Smad-2, TGF-1, TNF-, & IL-10 expression was significantly unaffected however Smad-4 and Smad-6 expression was increased. Compared to the untreated POI rats, our data indicated that the number of litters increased noticeably following AF-Exos. These findings imply that in POI rats, AF-Exos transplantation may be able to reestablish ovarian function via activating the TGF-/Smads signalling system [21].

Premature ovarian failure (POF), additionally referred to at primary ovarian insufficiency (POI), is the term for the loss or ovarian function in females following puberty before the age of 40 high serum gonadotropins and low oestrogen, periods that are not regular, amenorrhea, and diminished fertility. However, POF's particular pathophysiology is unknown, Its decreased ovarian tissue and impaired reserve function have no known treatment [22]. The most common stem cells used in regenerative medicine are mesenchymal stem cells (MSCs). have been extensively studied as well as in a variety of degenerative illnesses that have been tested to perform a proactive therapeutic function. MSCs have multidirectional differentiation potential as well as the capacity to self-renew, in addition to the release cytokines and exosomes [23].

MSCs may reverse POI and enhance the function of the ovarian reserve by differentiation into cells called granulosa (GCs), immunologic control, synthesis of cytokines together with additional nutritional factors, reduction of GCs apoptosis, or encouragement of GCs regeneration. MSCs have been shown in several

studies to have a regenerative effect on the structure and fertility of injured ovarian tissues, and they have recently emerged as a potent therapeutic approach for the treatment of individuals with POF. In the future, we want to totally reverse POI using MSC-based treatment [24].

Extracellular vesicles known as exosomes are distinguished in their size, source, mode of release, and contents. Single-stranded non-coding RNAs called microRNAs (miRNAs) are translated from DNA. Eukaryotic cells frequently contain exosomes and miRNAs, particularly mesenchymal stem cells (MSCs). MSCs have paracrine, anti-inflammatory, and immunomodulatory properties in addition to being employed for tissue regeneration. However, due to their potential to migrate and the growth factors they secrete, MSC usage is debatable, particularly when a tumour is present or after it has gone into remission. Compartments or substances produced from MSCs may be used as effective instruments for sickness diagnosis, follow-up, therapy, and monitoring intact MSCs. In this article, we go through a few features exosomal miRNAs produced by MSCs in the creation, characterization, and management of various disorders [25].

Women who have premature ovarian insufficiency (POI) experience considerable bodily harm and emotional strain. Exosome transplantation is a promising regenerative medicine technique that has the ability to effectively restore ovarian functioning on POI [26]. The study's objective is to evaluate the treatment efficiency of exosomes produced by hybrid umbilical vein mesenchymal stem cells (hUCMSC-Exos) in treating POI-related ovarian dysfunction as well as the contribution Using the Hippo pathway, exosome-mediated therapy. According to this study, Ovarian development and function were enhanced by hUCMSC-Exos through regulating the Hippo pathway. Exosomal transplantation may therefore represent a potential and effective therapeutic treatment for POI within the near future [27].

The multipotent cells found in large quantities in the human body are primed with special qualities that may be used in a broad variety of uses and remedies. Undifferentiated cells having the capacity to self-renew & specialise into a variety of lineages are known as mesenchymal stem cells (MSCs). depending on their origin [28]. MSCs are desirable candidates for cytotherapy in the treatment of a wide range of illnesses and ailments, particularly addition to being used in various facets of regenerative medicine, due to their demonstrated capacity to transmigrate towards sites of inflammation, the secretion of multiple substances that take part their role in tissue regeneration and immunoregulation [29]. MSCs, in particular, that are present in foetal, perinatal, or neonatal tissues, have extra qualities, such as a higher propensity for proliferation, an enhanced receptivity to environmental cues, and a reduced propensity to produce antibodies. Since numerous physiological processes are regulated by microRNA (miRNA)-guided gene regulation, the role of miRNAs in MSC development is becoming more and more clear. In this work, we investigate the mechanisms of miRNA-directed differentiation of mesenchymal stem cells (MSCs) with a focus on umbilical cord-derived mesenchymal stem cells (UCMSCs). The most significant miRNAs, miRNA sets, as signatures of miRNA are also identified [30].

5. Conclusion

This study sheds light on the unique microRNAs presents in uMSC-Exos and presents a novel strategy for utilising stem cell therapy to speed up wound healing and reduce scar formation. MicroRNAs in uMSC-Exos, such as miR-21, miR-23a, miR-125b, and miR-145, were found to inhibit TGF-b2, TGF-bR2, and SMAD2 activity, thereby decreasing collagen I deposition and suppressing alpha-smooth muscle actin (-SMA) expression through exosome-mediated intercellular transfer. This technique provides a promising alternative to traditional cell therapy by proposing that injecting wounds with modified uMSC-Exos containing transfected microRNAs can reduce scarring and improve patient outcomes. In addition to advancing our knowledge of microRNA-mediated wound healing, this discovery also paves the way for exciting new therapeutic approaches in the field of regenerative medicine.

Declarations

Ethics approval and consent to participate

Animal procedures described in this study have been approved by an institutionally authorized protocol from the Second Military Medical University Institute of Laboratory Animal Resources. Mature male Swiss-Hauschka ICR mice obtained from the Shanghai Laboratory Animal Research Centre (SIPPR-BK Laboratory Animal Corp., Shanghai, China) will be housed in a pathogen-free environment with 12-hour light-dark cycles and provided with unlimited access to standard chow and water. Prior to experimentation, mice will be anaesthetized with 10% chloral hydrate (0.3 ml/100 g) to ensure minimal discomfort. A uniform 1.5 cm diameter region of full-thickness dorsal skin will be surgically removed to induce skin defects. The wounds will be managed and monitored according to standard procedures, including coating with Tegaderm (3M, St. Paul, MN) for one day before removal. Passive extension and skin collection measurements will be taken on days 10, 14, and 25 to assess skin contracture. Hydro Matrix (Sigma-Aldrich, St. Louis, MO) will serve as a scaffold for the insertion of uMSC-Exoin, following the manufacturer's instructions. Separate preparations of a 100 mg/ml uMSC-Exo solution in phosphate-buffered saline (PBS) and a 1% (10 mg/ml) hydrogel in sterile water will be made and mixed in a 1:1 ratio for injection around the wound site 48 hours post-injury. Controls will include PBS, HEK-293-exosome (100 mg/ml), and uMSC exosome-free supernatant. Image analysis using Adobe Photoshop will be utilized to quantify wound healing progress at specific time points.

Consent for publication

Not Applicable

Funding

No founding received

Authors' information

Rongxia Lia, Xueping Liua, and Xiao Liangc contributed equally to this work (# denotes equal contribution). R.L., X.L., and X.L. were responsible for the conceptualization and design of the study.

Siling Tanga, Hongyan Xia, and Zi Xiua conducted the experiments and collected the data. Xinmiao Zhangc, Zhongyu Wuc, and Yancang Duanc,d,e analyzed and interpreted the results. R.L., X.L., and X.L. drafted the initial version of the manuscript. Xinmiao Zhangc prepared figures, and Yancang Duanc,d,e edited the manuscript for intellectual content. All authors, R.L., X.L., X.L., S.T., H.X., Z.X., X.Z., Z.W., and Y.D., contributed to the critical revision of the manuscript for important intellectual content. All authors approved the final version of the manuscript for submission.

References

1. Nisticò P, Bissell MJ, Radisky DC. Epithelial-mesenchymal transition: general principles and pathological relevance with special emphasis on the role of matrix metalloproteinases. Cold Spring Harb Perspect Biol. 2012;4(2):a011908.
2. Hay ED. An overview of epithelio-mesenchymal transformation. Cells Tissues Organs. 1995;154(1):8–20.
3. Micalizzi DS, Farabaugh SM, Ford HL. Epithelial-mesenchymal transition in cancer: parallels between normal development and tumor progression. J Mammary Gland Biol Neoplasia. 2010;15(2):117–34.
4. Kalluri R, Weinberg RA. The basics of epithelial-mesenchymal transition. J Clin Invest. 2009;119(6):1420–8.
5. Jeon H-M, Lee J. MET: roles in epithelial-mesenchymal transition and cancer stemness. Ann Transl Med. 2017;5(1):5.
6. Dennler S, Huet S, Gauthier JM. A short amino-acid sequence in MH1 domain is responsible for functional differences between Smad2 and Smad3. Oncogene. 1999;18:1643–8. 10.1038/sj.onc.1202729.
7. Itoh F, Asao H, Sugamura K, Heldin CH, ten Dijke P, Itoh S. Promoting bone morphogenetic protein signaling through negative regulation of inhibitory Smads. Embo J. 2001;20:4132–42. 10.1093/emboj/20.15.4132.
8. Watanabe M, Masuyama N, Fukuda M, Nishida E. Regulation of intracellular dynamics of Smad4 by its leucine-rich nuclear export signal. EMBO Rep. 2000;1:176–82. 10.1093/embo-reports/kvd029.
9. Tsukazaki T, Chiang TA, Davison AF, Attisano L, Wrana JL. SARA, a FYVE domain protein that recruits Smad2 to the TGFbeta receptor. Cell. 1998;95:779–91. 10.1016/S0092-8674(00)81701-8.
10. Massague J. How cells read TGF-beta signals. Nat Rev Mol Cell Biol. 2000;1:169–78. 10.1038/35043051.
11. Saitou M, Payer B, Lange UC, Erhardt S, Barton SC, Surani MA. Specification of germ cell fate in mice. Philos Trans R Soc Lond B Biol Sci. 2003;358:1363–70. 10.1098/rstb.2003.1324.
12. van den Hurk R, Zhao J. Formation of mammalian oocytes and their growth, differentiation and maturation within ovarian follicles. Theriogenology. 2005;63:1717–51. 10.1016/j.theriogenology.2004.08.005.

13. Lopes CdeS, van den Driesche SM, Carvalho S, Larsson RL, Eggen J, Surani B, Mummery MA. Altered primordial germ cell migration in the absence of transforming growth factor beta signaling via ALK5. Dev Biol. 2005;284:194–203. 10.1016/j.ydbio.2005.05.019.
14. Hanrahan JP, Gregan SM, Mulsant P, Mullen M, Davis GH, Powell R, Galloway SM. Mutations in the genes for oocyte-derived growth factors GDF9 and BMP15 are associated with both increased ovulation rate and sterility in Cambridge and Belclare sheep (Ovis aries). Biol Reprod. 2004;70:900–9. 10.1095/biolreprod.103.023093.
15. Yi SE, LaPolt PS, Yoon BS, Chen JY, Lu JK, Lyons KM. The type I BMP receptor BmprIB is essential for female reproductive function. Proc Natl Acad Sci U S A. 2001;98:7994–9. 10.1073/pnas.141002798.
16. Ding C, Zou Q, Wang F, Wu H, Wang W, Li H, Huang B. HGF and BFGF Secretion by Human Adipose-Derived Stem Cells Improves Ovarian Function During Natural Aging via Activation of the SIRT1/FOXO1 Signaling Pathway. Cell Physiol Biochem. 2018;45:1316–32.
17. Ding L, Li X, Sun H, Su J, Lin N, Péault B, Song T, Yang J, Dai J, Hu Y. Transplantation of bone marrow mesenchymal stem cells on collagen scaffolds for the functional regeneration of injured rat uterus. Biomaterials. 2014;35:4888–900.
18. Ding C, Li H, Wang Y, Wang F, Wu H, Chen R, Lv J, Wang W, Huang B. Different therapeutic effects of cells derived from human amniotic membrane on premature ovarian aging depend on distinct cellular biological characteristics. Stem Cell Res Ther. 2017;8:173.
19. Huang B, Lu J, Ding C, Zou Q, Wang W, Li H. Exosomes derived from human adipose mesenchymal stem cells improve ovary function of premature ovarian insufficiency by targeting SMAD. Stem Cell Res Ther. 2018;9(1):216. 10.1186/s13287-018-0953-7. PMID: 30092819; PMCID: PMC6085638.
20. Nazdikbin Yamchi N, Ahmadian S, Mobarak H, Amjadi F, Beheshti R, Tamadon A, Rahbarghazi R, Mahdipour M. Amniotic fluid-derived exosomes attenuated fibrotic changes in POI rats through modulation of the TGF-β/Smads signaling pathway. J Ovarian Res. 2023;16(1):118. 10.1186/s13048-023-01214-1. PMID: 37370156; PMCID: PMC10294370.
21. Shi L, Zhang Z, Deng M, Zheng F, Liu W, Ye S. Biological mechanisms and applied prospects of mesenchymal stem cells in premature ovarian failure. Med (Baltim). 2022;101(32):e30013. 10.1097/MD.0000000000030013. PMID: 35960112; PMCID: PMC9371578.
22. Wolf P. The nature and significance of platelet products in human plasma. Br J Haematol. 1967;13(3):269–88.
23. Caruso S, Poon IKH. Apoptotic cell-derived extracellular vesicles: more than just debris. Front Immunol. 2018;9:1486.
24. Tricarico C, Clancy J, D'Souza-Schorey C. Biology and biogenesis of shed microvesicles. Small GTPases. 2017;8(4):220–32.
25. Hessvik NP, Llorente A. Current knowledge on exosome biogenesis and release. Cell Mol Life Sci. 2018;75(2):193–208.
26. Li Z, Zhang M, Zheng J, Tian Y, Zhang H, Tan Y, Li Q, Zhang J, Huang X. Human Umbilical Cord Mesenchymal Stem Cell-Derived Exosomes Improve Ovarian Function and Proliferation of Premature

Ovarian Insufficiency by Regulating the Hippo Signaling Pathway. Front Endocrinol (Lausanne). 2021;12:711902. 10.3389/fendo.2021.711902. PMID: 34456868; PMCID: PMC8397419.

27. Bottini S, Hamouda-Tekaya N, Mategot R, Zaragosi LE, Audebert S, Pisano S, Grandjean V, Mauduit C, Benahmed M, Barbry P, et al. Post-transcriptional gene silencing mediated by microRNAs is controlled by nucleoplasmic Sfpq. Nat Commun. 2017;8:1189.
28. Paul P, Chakraborty A, Sarkar D, Langthasa M, Rahman M, Bari M, Singha RS, Malakar AK, Chakraborty S. Interplay between miRNAs and human diseases. J Cell Physiol. 2018;233:2007–18. [.
29. Collino F, Bruno S, Deregibus MC, Tetta C, Camussi G. MicroRNAs and mesenchymal stem cells. Vitam Horm. 2011;87:291–320.
30. Yang C, Luo M, Chen Y, You M, Chen Q. MicroRNAs as Important Regulators Mediate the Multiple Differentiation of Mesenchymal Stromal Cells. Front Cell Dev Biol. 2021;9:619842.

Supplementary data file

Supplementary data file is not available with this version.

Figures

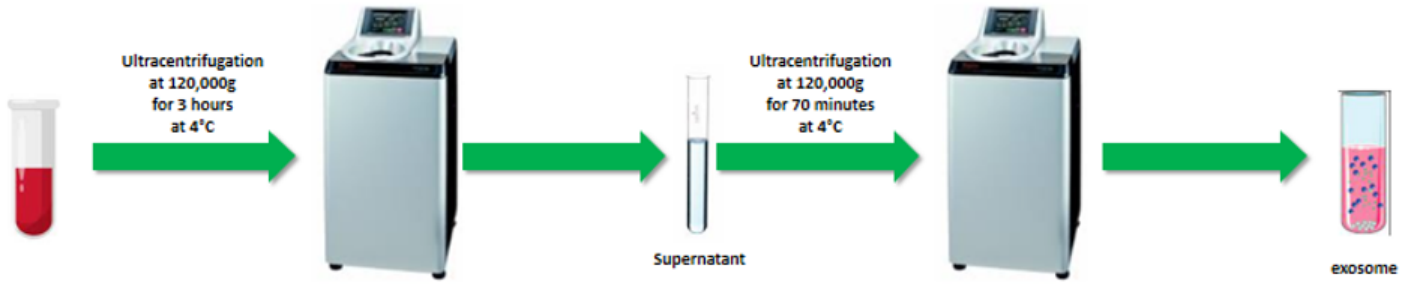

Figure 1

Process of exosome Isolation

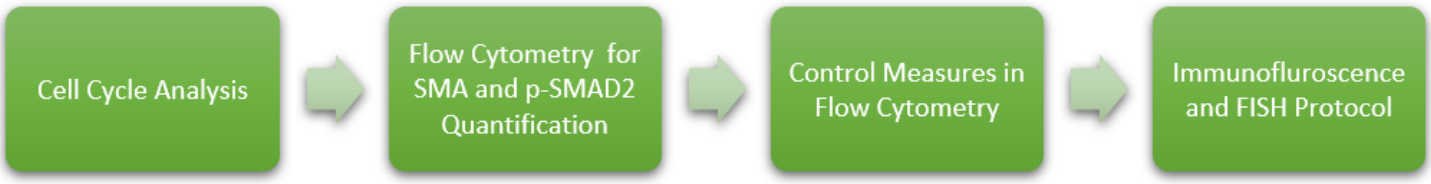

Figure 2

Summary of the Cell Cycle analysis and FISH protocol

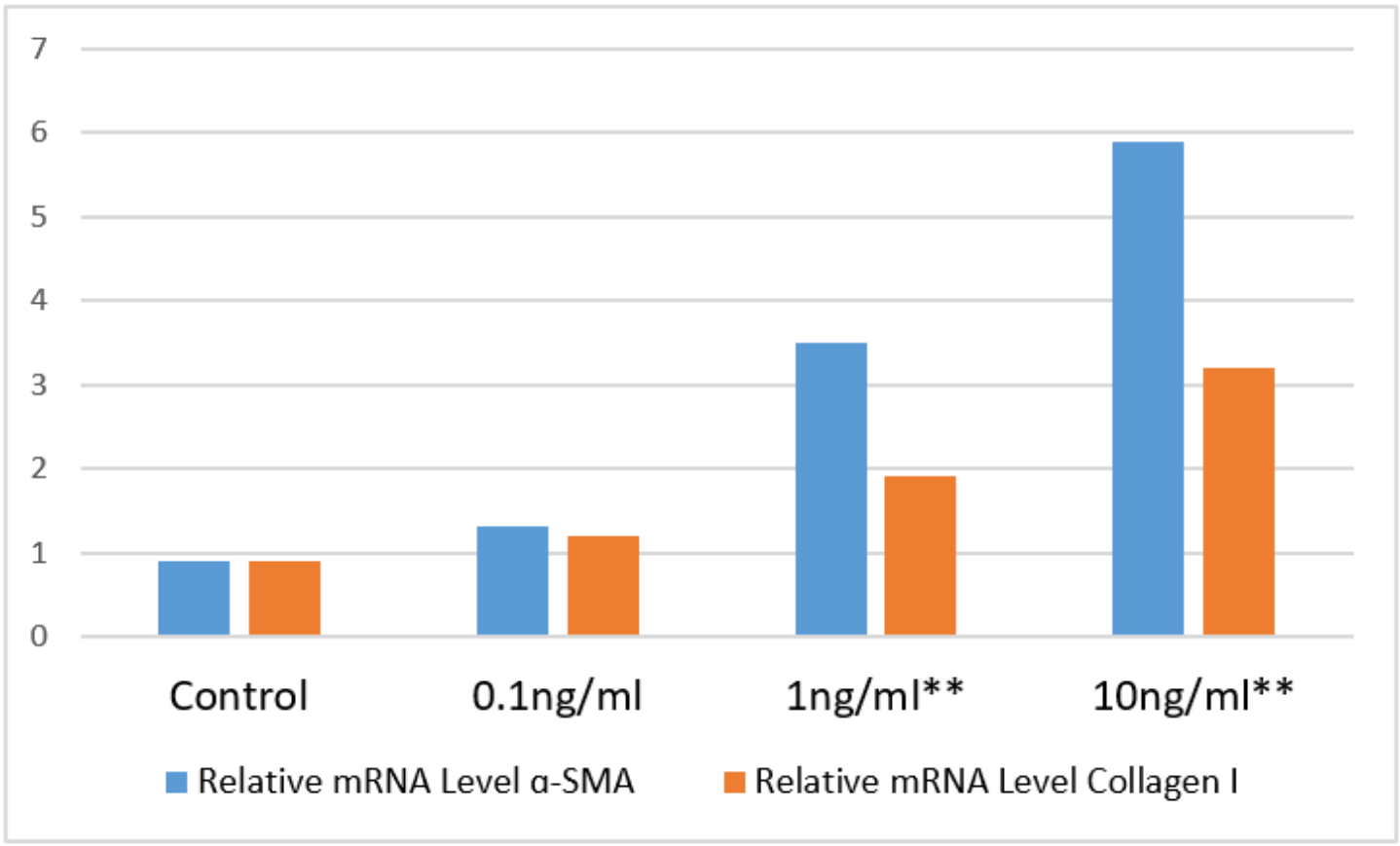

Figure 3

-SMA and Collagen I expressionat different TGF-β1 dosages (** indicates p<0.05)

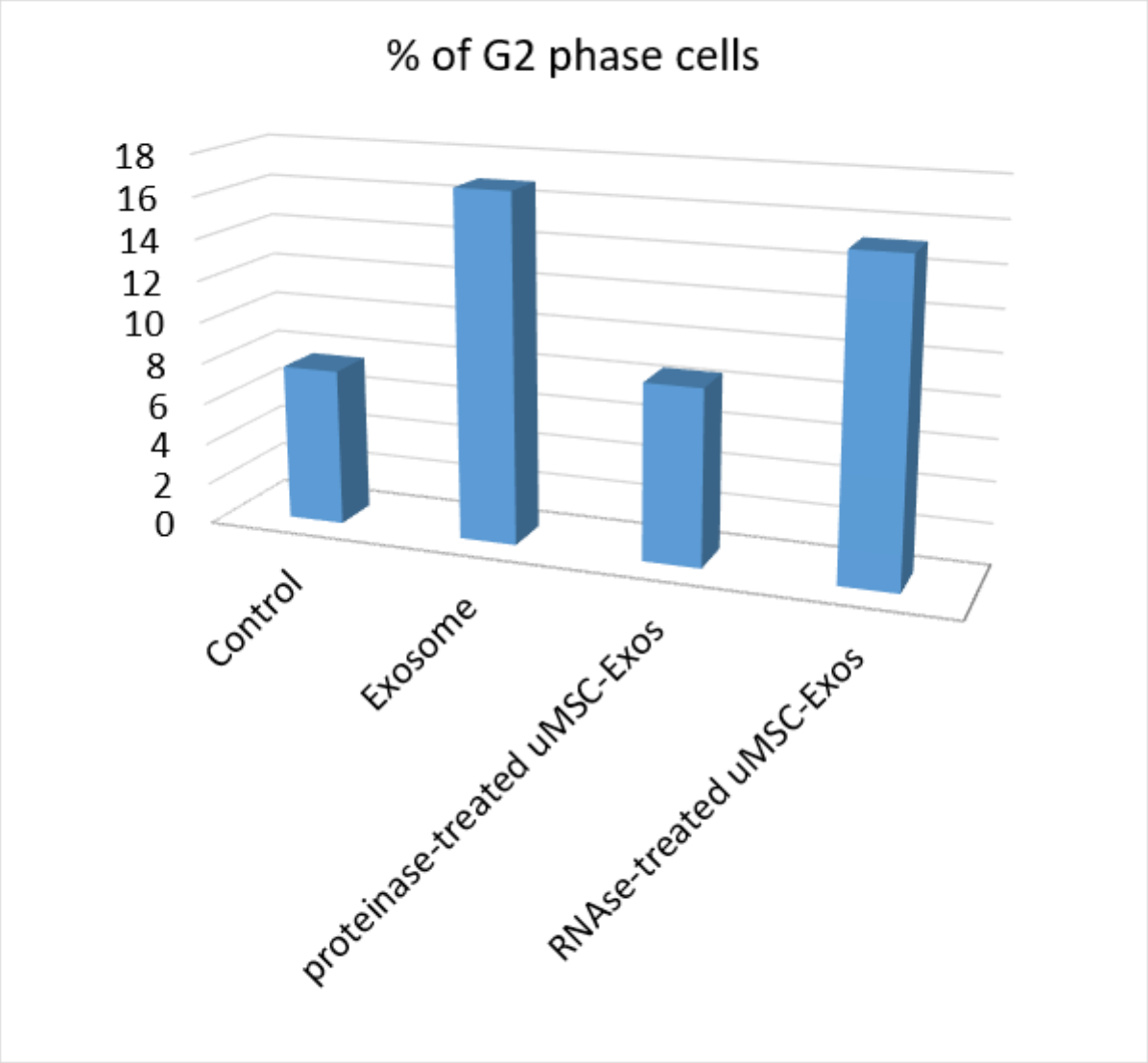

Figure 4

Cell cycle analysis of different enzyme-treated exosomes

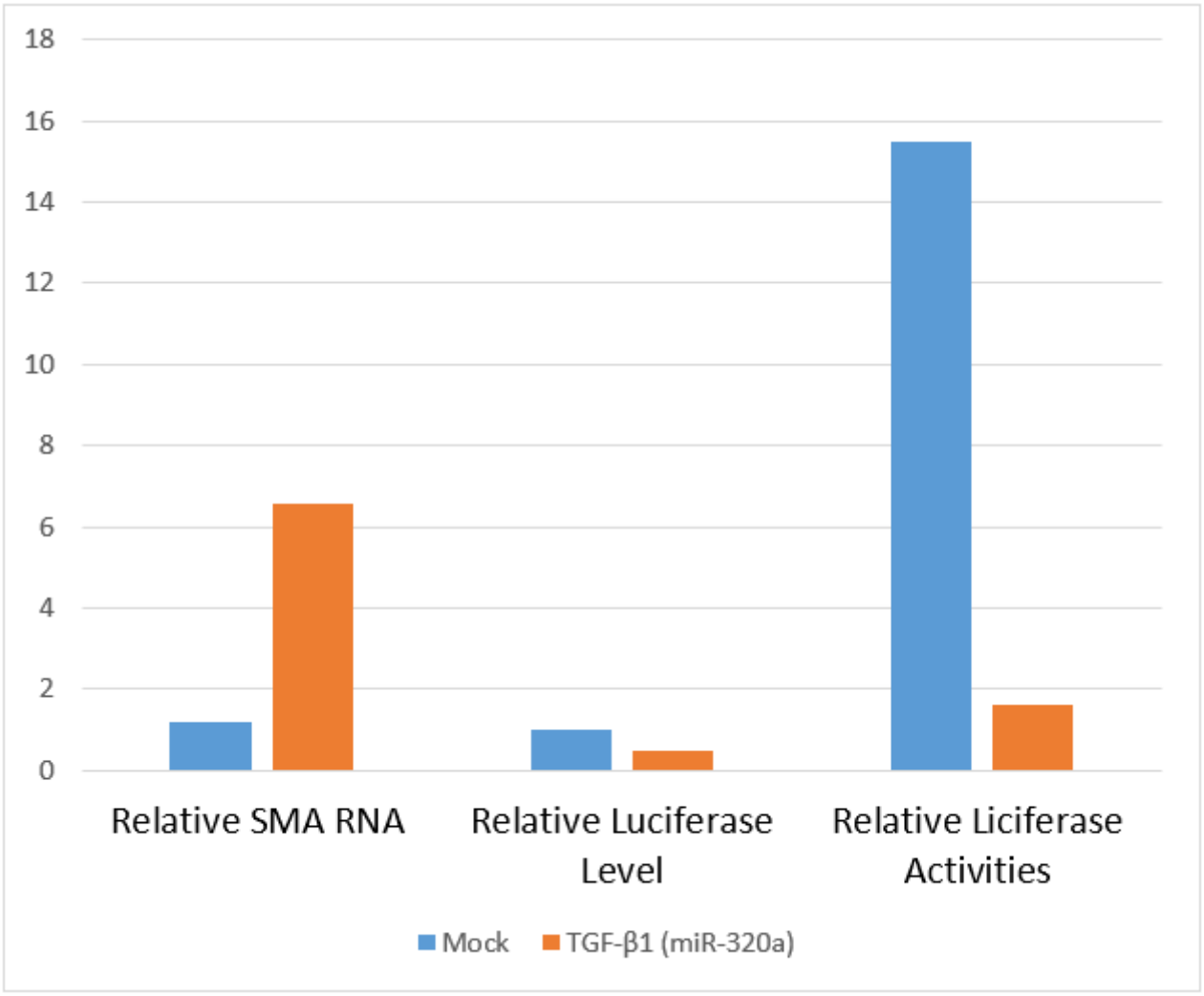

Figure 5

Binding sites of uMSC-Exo-specific miRNAs and their respective targets. Results of Luciferase Reporter Assay showing luciferase activities. SMAD2 Reporter analysis revealing luciferase level of SMAD2-binding sequence